Short communication

Catalytic activity of graphene–cobalt hydroxide composite for oxygen reduction reaction in alkaline media

Jiajia Wu [a,b], Dun Zhang [a,*], Yi Wang [a], Yi Wan [a,b], Baorong Hou [a]

[a] Shandong Provincial Key Laboratory of Corrosion Science, Institute of Oceanology, Chinese Academy of Sciences, Qingdao 266071, China
[b] Graduate School of the Chinese Academy of Sciences, Beijing 100039, China

ABSTRACT

The electrocatalysis of graphene–cobalt hydroxide ($Co(OH)_2$) composite towards oxygen reduction reaction (ORR) in 0.1 M KOH is studied with $Co(OH)_2$/graphene-modified glassy carbon (GC) electrode using cyclic and rotating ring-disk electrode voltammetry. The electrode is prepared by casting of graphene suspension on GC electrode and subsequent electrodeposition of $Co(OH)_2$ from $Co(NO_3)_2$ solution. A characteristic interlaced nanowalls morphology is observed for $Co(OH)_2$ with scanning electron microscopy. Raman spectra demonstrate the microstructure of graphene changes during electrochemical treatment in nitrate solutions, which has a great impact on its catalysis towards ORR. At GC electrode, two reduction processes both attributed to 2-electron reduction are recorded for ORR. The presence of $Co(OH)_2$ on GC electrode results in larger peak current without obvious potential shift due to its good catalytic activity towards the disproportionation of intermediates. Graphene not only increases the peak current and shifts the peak potential in the positive direction, but also leads to further reduction of HO_2^- at the second step. After electrochemical treatment in nitrate solutions, graphene is activated to catalyze the disproportionation of HO_2^- effectively, and its cooperation with $Co(OH)_2$ enables reduction of O_2 to OH^- at lower overpotential. Graphene–$Co(OH)_2$ composite is a potential electrode material for air cathodes in alkaline electrolyte electrochemical systems.

© 2011 Elsevier B.V. All rights reserved.

1. Introduction

Interest in alkaline fuel cells has been resurging in recent years, due to the alleviation of carbon dioxide poisoning problem with the development of anion exchange membrane [1]. As a low-temperature energy conversion technology, the sluggish oxygen reduction reaction (ORR) at the cathode decreases energy efficiency and power density. Thus, catalysts with high activity towards ORR are highly desirable. Pt and Pt-based alloys are still the most widely used catalysts for ORR in acid fuel cells for their excellent catalytic activity and stability, but the less corrosive alkaline electrolyte allows the use of non-Pt metals. Until now, many promising non-Pt catalysts have been reported, such as silver [2], manganese oxide and their combination with metal macrocyclic complex or carbon nanotube (CNT) [3–5], nonprecious-metal chalcogenides [6,7], Fe- or Co-based catalysts [8], and nitrogen-doped CNT [9,10].

Graphene, a novel carbon nanomaterial with unique physical and chemical properties, has a good potential in electrochemical application. It has been reported that graphene can be used in electrochemical sensors [11,12], capacitors [13,14], lithium batteries [15,16], solar cells [17], and catalysts for fuel oxidation [18,19]. There are also many reports on its utilization in ORR, either as catalyst support material or as catalyst itself. When used as support material, the supported catalysts are usually precious metals, like Pt, Au, Pd, and their alloys [20–23]. The presence of graphene results in better dispersion of active catalysts and thus improves the catalytic activity and durability [22]. Unlike precious metal catalysts, few studies are concerned about the combination of graphene with non-precious ORR catalysts. When used as catalyst itself, nitrogen-doped graphene is focused due to the fact that the introduction of nitrogen heteroatom creates active site for reduction of O_2 [24–26]. However, the synthesis of nitrogen-doped graphene usually involves chemical vapor deposition [27], nitrogen plasma treatment [28], arc discharge in the presence of protective gases and nitrogen source vapor [29], or high temperature treatment in ammonia [30]. These methods increase the cost and complicate the operation in comparison with chemical reduction of graphite oxide (GO).

In our previous work, we have studied the catalytic activity of graphene synthesized via hydrazine reduction of GO and cobalt hydroxide ($Co(OH)_2$) prepared by galvanostatic electrodeposition towards ORR [31,32]. Both materials show good catalytic activity, in which graphene decreases the reaction overpotential and $Co(OH)_2$ catalyzes the disproportionation of intermediates. Inspired by this,

* Corresponding author. Tel.: +86 532 82898960; fax: +86 532 82898960.
E-mail address: zhangdun@qdio.ac.cn (D. Zhang).

we attempted to prepare a composite of graphene and $Co(OH)_2$ as ORR catalyst in this study and reduction of O_2 to OH^- did occur at low overpotential in 0.1 M KOH. Furthermore, it was found that graphene could be activated during the potentiostatic electrodeposition of $Co(OH)_2$, and the activated graphene can catalyze the disproportionation of peroxide (HO_2^-), which has not been reported before. To our best knowledge, this is the first report on the catalysis of graphene–$Co(OH)_2$ composite towards ORR.

## 2. Experimental

2.1. Chemicals and materials

For synthesis of graphene, natural graphite powder (99.99%) was purchased from Beijing Chemical Company (China) and reagents including H_2SO_4 (98%), $NaNO_3$, $KMnO_4$, H_2O_2 (30%), $N_2H_4 \cdot H_2O$ (85%), and $NH_3 \cdot H_2O$ (28%) with analytical grade were provided by Sinopharm Chemical Reagent Co. Ltd. (China). $Co(NO_3)_2$ and KOH were utilized to prepare solutions for electrodeposition of $Co(OH)_2$ and electrochemical measurements. Ultra-high purity N_2 and O_2 (Heli Gas Co. Ltd., China) were used for the deaeration of solutions and the preparation of O_2-saturated solutions, respectively. All aqueous solutions were prepared with Milli-Q water (Millipore, USA).

2.2. Synthesis of graphene

Graphene was synthesized via chemical reduction of GO. GO was made by a modified Hummers method [33], which consists of pre-oxidation of natural graphite with concentrated H_2SO_4 and $KMnO_4$, re-oxidation with H_2O_2, and exfoliation by sonication. Then, the chemical reduction of GO was carried out according to the method reported by Li et al. [34]. In brief, 10 mL of GO dispersion with a concentration of $0.5\,mg\,mL^{-1}$ was mixed with 70 μL $NH_3 \cdot H_2O$ (28%) and 4 μL $N_2H_4 \cdot H_2O$ (85%) in a 20 mL glassy vial. After being stirred for 5 min, the vial was put in a water bath (95 °C) for 1 h to obtain graphene dispersion.

2.3. Preparation of modified glassy carbon (GC) electrodes

A rotating ring-disk electrode (RRDE, Pine Research Instrument Inc., USA) with a GC disk (5.61 mm diameter) and a Pt ring (7.92 mm outer diameter and 6.25 mm inner diameter) was used in this study. Prior to the surface modification, the disk electrode was polished with 1.0 and 0.05 μm alumina slurries, and then cleaned by sonication for 15 min. A graphene modified GC (graphene/GC) electrode was prepared by casting the graphene suspension on the disk electrode surface and drying in N_2 atmosphere at ambient temperature. The loading of graphene on the surface of GC electrode was ca. $0.04\,mg\,cm^{-2}$. $Co(OH)_2$ was electrodeposited on the graphene/GC or bare GC electrode by applying a potential of -1.1 V vs. Ag/AgCl (KCl-sat.) for 30 s in 10 mM $Co(NO_3)_2$ solution. The deposition of $Co(OH)_2$ can be expressed by the following reactions:

$$NO_3^- + 7H_2O + 8e^- \rightarrow NH_4^+ + 10OH^- \tag{I}$$

$$Co^{2+} + 2OH^- \rightarrow Co(OH)_2 \tag{II}$$
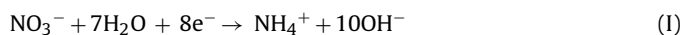
Cathodic reduction of NO_3^- results in the electrogeneration of OH^- (reaction (I)), which causes a steep increase in the pH close to the electrode surface, and then $Co(OH)_2$ precipitation takes places (reaction (II)). To investigate whether the catalytic activity of graphene was affected by electrodeposition process, we also treated the graphene/GC electrode in 20 mM $NaNO_3$ solution in the same manner.
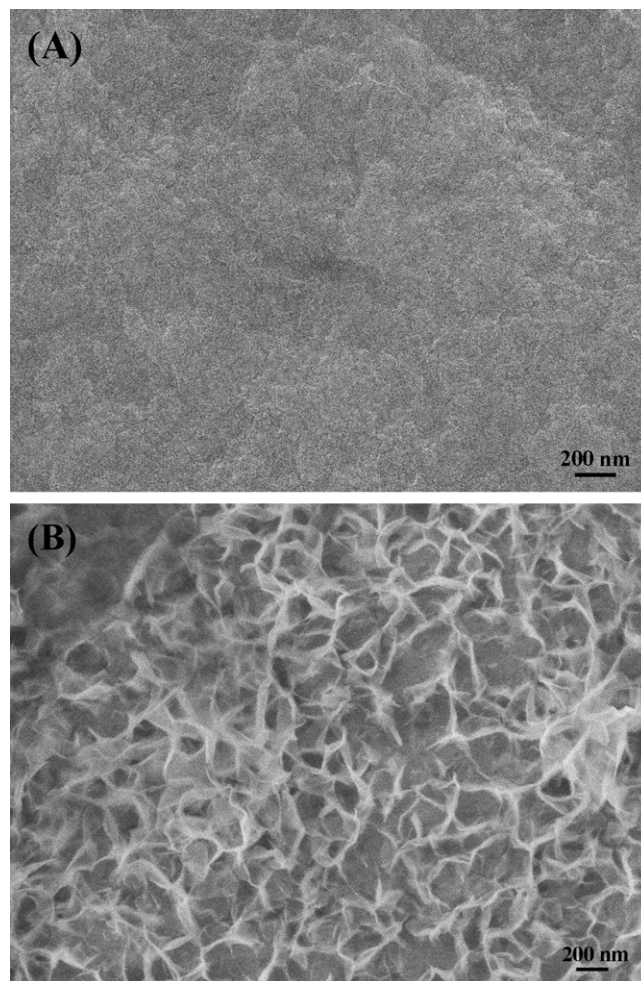

Fig. 1. SEM images of graphene/GC (A) and $Co(OH)_2$/graphene/GC (B) electrodes.

2.4. Electrochemical, scanning electron microscopic, and Raman spectroscopic measurements

Cyclic and RRDE voltammetric electrochemical measurements were performed on a computer-controlled electrochemical analyzer (CHI 760C, CH Instruments, Inc., USA) with a three-electrode electrochemical cell. A Pt wire and a Ag/AgCl (KCl-sat.) electrode were used as the counter electrode and reference electrode, respectively. The working electrodes consisted of GC, graphene/GC, $Co(OH)_2$/GC, $Co(OH)_2$/graphene/GC, and $NaNO_3$-treated graphene/GC disk electrodes and Pt ring electrode. In RRDE measurement, Pt ring electrode was kept at +0.5 V to determine HO_2^- produced at the disk electrode. All potentials are reported vs. the Ag/AgCl (KCl-sat.) electrode. A JOEL JSM-6700F scanning electron microscope (SEM) was employed for morphology observation and Raman Spectra were obtained using a Jobin-Yvon LabRam-Infinity system. All experiments were carried out at room temperature (25 °C).

3. Results and discussion

3.1. SEM images and Raman spectra of modified GC electrodes

SEM images of graphene/GC and $Co(OH)_2$/graphene/GC electrodes are shown in Fig. 1. The graphene film made of many stacked graphene layers exhibits a rough structure, which is an ideal support for depositing nanomaterials. For $Co(OH)_2$ electrodeposited on the surface of graphene film, a characteristic interlaced nanowalls
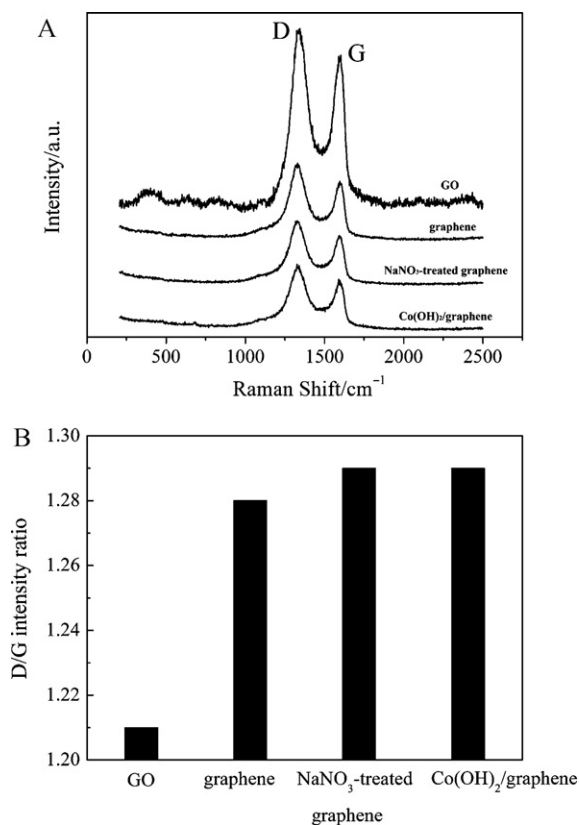
Fig. 2. (A) Raman spectra of GO, graphene, NaNO₃-treated graphene, and Co(OH)₂/graphene. The corresponding D/G intensity ratios are shown in (B).

Fig. 3. CVs recorded at bare GC (a and a′), Co(OH)₂/GC (b and b′), graphene/GC (c and c′), NaNO₃-treated graphene/GC (d and d′), and Co(OH)₂/graphene/GC (e and e′) electrodes in N₂- (a′, b′, c′, d′, and e′) and O₂-saturated (a, b, c, d, and e) 0.1 M KOH solutions. Scan rate: 50 mV s^{-1}.

of O_2 to HO_2^-, the first of which is mediated by the active native surface quinone-like groups with superoxide anion ($O_2^{\bullet-}$) as the intermediate (reactions (III)–(VI)), while the second is a direct 2-electron reduction (reaction (VII)) at the GC surface [41].

$$Q + e^- \rightarrow Q^{\bullet-} \tag{III}$$

$$Q^{\bullet-} + O_2 \rightarrow Q + O_2^{\bullet-} \tag{IV}$$

$$2O_2^{\bullet-} + H_2O \rightarrow HO_2^- + O_2 + OH^- \tag{V}$$

$$O_2^{\bullet-} + H_2O + e^- \rightarrow HO_2^- + OH^- \tag{VI}$$

$$O_2 + H_2O + 2e^- \rightarrow HO_2^- + OH^- \tag{VII}$$

The modification of Co(OH)₂ on GC electrode does not yield any cyclic voltammetric waves in N₂-saturated solution (curve b′), demonstrating that Co(OH)₂ in this system is electro-inactive in the potential window employed. However, in O₂-saturated solution, the presence of Co(OH)₂ greatly increases the current of these two cathodic peaks without obvious potential shifts (curve b), indicating Co(OH)₂ possesses excellent catalytic activity for the disproportionation of $O_2^{\bullet-}$ (reaction (V)) and HO_2^- (reaction (VIII)), which is in good agreement with our previous report [32].

$$2HO_2^- \rightarrow 2OH^- + O_2 \tag{VIII}$$

Different from bare GC electrodes, there is a pair of reversible redox peaks (indicated by two vertical arrows) at ca. −0.40 V on the graphene/GC electrode in N₂-saturated solution (curve c′), which can be ascribed to the quinone-like groups [42]. At such an electrode, ORR also undergoes two processes (curve c). The first reduction peak at ca. −0.25 V is essentially redox-mediated by the quinone-like groups at graphene (reaction (III)–(VI)). The modification of graphene on GC electrode greatly increases the peak current and makes the peak potential shift by ca. 130 mV towards the positive direction. The second peak at ca. −0.88 V corresponds to further reduction of HO_2^- produced to OH^- (reaction (IX)) as will be evident with RRDE voltammetry shown below.

$$HO_2^- + 2e^- + H_2O \rightarrow 3OH^- \tag{IX}$$

In N₂-saturated 0.1 M KOH, the CV of Co(OH)₂/graphene/GC electrode (curve e′) is similar to that of graphene/GC electrode. But the CVs of these two electrodes obtained in O₂-saturated solution are totally different. The presence of Co(OH)₂ on graphene/GC electrode leads to an increase in the first reduction peak current of O_2 to HO_2^- (reaction (III)–(VI)) and a clear decrease in the second reduction peak current of HO_2^- to OH^- (reaction (IX), curve e). Furthermore, the peak potential shifts from −0.25 V to −0.20 V. However, it has been mentioned above that Co(OH)₂ increases the

morphology is observed, which provides easy access of O_2 to the underlying graphene. In comparison with the morphology of electrodeposited Co(OH)₂ reported by others [35,36], ours seems not so regular, which may be associated with the absence of surfactants and different substrates. The presence of Co element in energy dispersive spectrometer spectrum (data not shown here) confirms the successful preparation of Co(OH)₂ again.

Raman spectroscopy is a powerful nondestructive tool to distinguish ordered and disordered crystal structures of carbon. G band is usually assigned to the E_{2g} phonon of sp² atoms, while D band is a breathing mode of κ-point phonons of A_{1g} symmetry [37]. Fig. 2 depicts Raman spectra of GO, graphene, Co(OH)₂/graphene, and NaNO₃-treated graphene and the corresponding D/G intensity ratios are also shown. The spectra of these four materials are similar, which all contain D band at wavenumber of ca. 1340 cm^{-1} and G band at ca. 1595 cm^{-1}. But the D/G intensity ratio increases from 1.21 of GO to 1.28 of graphene, and further rises to 1.29 after electrochemical treatment by applying a potential of −1.1 V for 30 s in 10 mM Co(NO₃)₂ or 20 mM NaNO₃ solution. This change suggests a decrease in the average size and an increase in the number of small crystalline graphitic domains, which is consistent with the results of some reports on chemical and electrochemical reduction of GO [38–40]. As shown below, this microstructure change in graphene has a great impact on its catalytic activity towards ORR.

3.2. Cyclic voltammetry for O_2 reduction

Cyclic voltammograms (CVs) for O_2 reduction obtained at bare GC, Co(OH)₂/GC, graphene/GC, Co(OH)₂/graphene/GC, and NaNO₃-treated graphene/GC electrodes are shown in Fig. 3. Compared with N₂-saturated 0.1 M KOH (curve a′), there are two cathodic peaks at ca. −0.38 V and −0.84 V on bare GC electrode in O₂-saturated solution (curve a). Both processes are attributed to 2-electron reduction
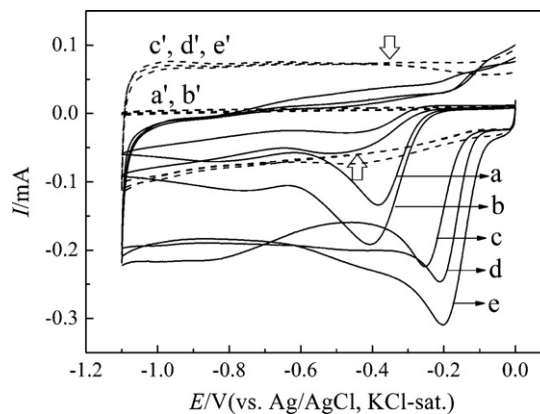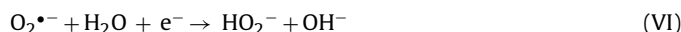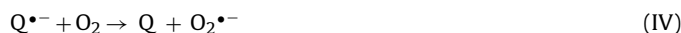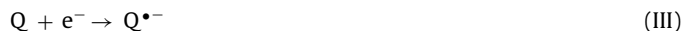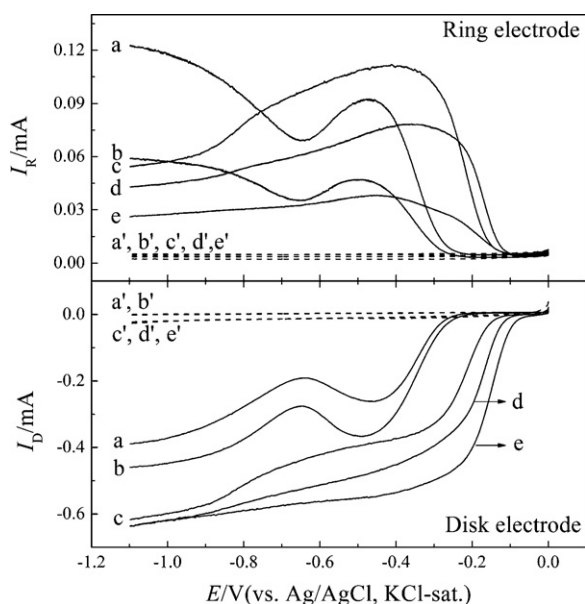
Fig. 4. RRDE voltammograms with a rotation rate of 400 rpm at bare GC- (a and a′), Co(OH)₂/GC- (b and b′), graphene/GC- (c and c′), NaNO₃-treated graphene/GC- (d and d′), and Co(OH)₂/graphene/GC-Pt (e and e′) electrodes in N₂- (a′, b′, c′, d′, and e′) and O₂-saturated (a, b, c, d, and e) 0.1 M KOH solutions. Scan rate: 10 mV s⁻¹.

current without potential shifts. What will be responsible for the positive potential shift of the first peak? The change of graphene during electrodeposition of Co(OH)₂ should be responsible, and this can be confirmed by CVs on NaNO₃-treated graphene/GC electrode. Based on the data available, the change mainly refers to microstructure variation mentioned above.

In comparison with 10 mM Co(NO₃)₂, applying a potential of −1.1 V on graphene/GC electrode in 20 mM NaNO₃ could not cause the precipitation of Co(OH)₂ on the electrode surface, but it could also induce the microstructure variation of graphene with an increase of D/G intensity ratio (shown in Fig. 2B). After electrochemical treatment in NaNO₃ solution, the first peak potential shifts to −0.20 V (curve d), indicating graphene is activated during the electrochemical treatment, and the activated graphene decreases the reaction overpotential. Interestingly, besides the positive shift of peak potential, the current response for ORR on NaNO₃-treated graphene/GC electrode is similar to that on Co(OH)₂/graphene/GC electrode except for a smaller peak current. Therefore, the activated graphene also catalyzes the disproportionation of HO₂⁻. The O₂ replenished from reaction (VIII) could be re-reduced, resulting in the increase in the first reduction peak current of reaction (III)–(VI) and the decrease in the second peak current of reaction (IX). On the Co(OH)₂/graphene/GC electrode, current for the peak at ca. −0.20 V increases further due to the catalytic activity of Co(OH)₂ towards O₂•⁻ and HO₂⁻ disproportionation.

3.3. RRDE voltammetry for O₂ reduction

The RRDE voltammograms for O₂ reduction obtained at bare GC, Co(OH)₂/GC, graphene/GC, Co(OH)₂/graphene/GC, and NaNO₃-treated graphene/GC disk electrodes and Pt ring electrode are shown in Fig. 4. Similar to the results of cyclic voltammetry, two reduction processes are recorded at bare GC disk electrode, and the corresponding ring current exhibits two typical steps ascribed to both 2-electron reduction of O₂ to HO₂⁻ (curve a) [43]. Electrodeposition of Co(OH)₂ on GC disk electrode clearly results in a larger disk current for O₂ reduction and a smaller ring current for HO₂⁻ oxidation (curve b), further confirming that Co(OH)₂ possesses good catalytic activity for HO₂⁻ disproportionation. Two

reduction steps are also observed on graphene/GC disk electrode (curve c), but the modification of graphene leads to an significant increase in disk current and ca. 130 mV positive shift of the half-wave potential. Furthermore, very different from bare GC electrode, the second reduction process on the graphene/GC disk electrode is attributed to the reduction of HO₂⁻, which is supported by the decrease in ring current. After electrochemical treatment in 20 mM NaNO₃ solution, it is not that easy to tell the second reduction process on graphene modified GC electrode (curve d), deriving from the disproportionation of HO₂⁻ induced by activated graphene. The disproportionation of HO₂⁻ provides additional O₂ for the first reduction step, and decreases the amount of HO₂⁻ for further reduction at the second step. Consequently, the current interval between these two stages is much smaller than that on graphene/GC disk electrode. The deposited Co(OH)₂ further enhances the disproportionation of HO₂⁻, as a result, only one reduction step is observed on Co(OH)₂/graphene/GC electrode (curve e). In comparison with bare GC electrode, the half-wave potential for O₂ reduction on the Co(OH)₂/graphene/GC electrode is shifted ca. 190 mV in the positive direction, and also the reduction current increases obviously. These results demonstrate that our graphene–Co(OH)₂ composite possesses good catalytic activity towards ORR.

On the basis of RRDE voltammograms, we can calculate the number of electrons transferred (n) and percentage of HO₂⁻ (% HO₂⁻) for ORR. The equations used are [44,45]:

$$n = \frac{4I_D}{(I_D + I_R/N)} \tag{1}$$

$$\%\ HO_2^- = \frac{100(2I_R/N)}{(I_D + I_R/N)} \tag{2}$$

where I_D and I_R denote the faradic current at the disk and ring electrode, respectively, which are deduced by subtraction of the current in N₂-saturated 0.1 M KOH, and N, collection efficiency, is taken as 0.37 for our experiment. The potential dependences of calculated n and % HO₂⁻ are shown in Fig. 5. It can be seen from Fig. 5A that the value of n on bare GC electrode remains at round 2 in the potential window employed (curve a), and the introduction of Co(OH)₂ results in its increase to greater than 3 (curve b), which is in accordance with the properties of Co(OH)₂ mentioned above. For graphene/GC electrode (curve c), the n value is close to 2 at low overpotentials ($E > −0.4$ V) and gradually increases ($n > 3$ at −0.9 V), suggesting HO₂⁻ produced reduces to OH⁻ at more negative potentials. The electrochemical activation of graphene/GC electrode in 20 mM NaNO₃ causes a higher n value, and the value can reach to 3 at −0.6 V (curve d), which confirms that activated graphene does catalyze the disproportionation of HO₂⁻ effectively. The value of n on Co(OH)₂/graphene/GC reaches 3.5 at quite low overpotentials due to the synergistic effect of activated graphene and Co(OH)₂ (curve e), indicating the prepared graphene–Co(OH)₂ composite has high catalytic activity towards reduction of O₂ to OH⁻. As shown in Fig. 5B, the value of % HO₂⁻ on bare GC and Co(OH)₂/GC electrodes changes minimally with potential (curves a and b), and the introduction of Co(OH)₂ induces a decrease of the value from greater than 90 to ca. 45. Different from bare GC electrode, the % HO₂⁻ value on graphene/GC electrode is dependent on potential (curve c), in which it is higher than 80 at potentials for the first reduction step and drops to ca. 40 at potentials more negative than −0.9 V. This difference is attributed to the occurrence of HO₂⁻ reduction rather than the direct 2-electron reduction of O₂ at the second step on graphene/GC electrode. After electrochemical treatment in 20 mM NaNO₃, the value of % HO₂⁻ decreases obviously (curve d), and further precipitation of Co(OH)₂ results in a value of ca. 20 (curve e), which is accordance with our prediction
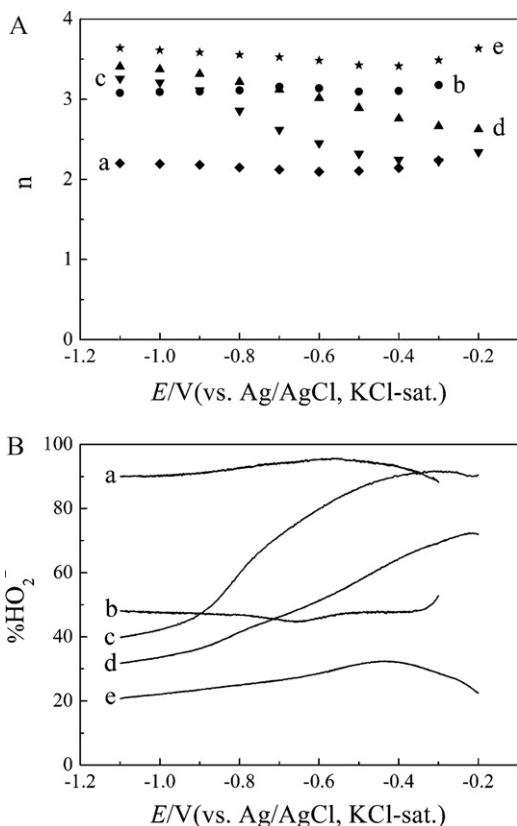
A

B

Fig. 5. The dependence of n (A) and % HO_2^- (B) on potential.

on the catalytic activity of activated graphene and $Co(OH)_2$ towards HO_2^- disproportionation.

4. Conclusions

We have first demonstrated that graphene–$Co(OH)_2$ composite possesses excellent catalytic activity for reduction of O_2 to OH^- in 0.1 M KOH. At graphene modified GC electrode, O_2 reduction undergoes two successive 2-electron processes with HO_2^- as intermediate. After electrochemical treatment in 10 mM $Co(NO_3)_2$, not only precipitation of $Co(OH)_2$ but also activation of graphene occurs. The activated graphene decreases the overpotential and catalyzes the disproportionation of HO_2^-, and its combination with $Co(OH)_2$ results in 4-electron O_2 reduction at lower overpotential. The present work enriches the ORR catalysts.

References

[1] X.G. Li, B.N. Popov, T. Kawahara, H. Yanagi, J. Power Sources 196 (2011) 1717.
[2] N. Wagner, M. Schulze, E. Gülzow, J. Power Sources 127 (2004) 264.
[3] L.Q. Mao, D. Zhang, T. Sotomura, K. Nakatsu, N. Koshiba, T. Ohsaka, Electrochim. Acta 48 (2003) 1015.
[4] D. Zhang, D.H. Chi, T. Okajima, T. Ohsaka, Electrochim. Acta 52 (2007) 5400.
[5] D. Zhang, T. Sotomura, T. Ohsaka, Chem. Lett. 35 (2006) 520.
[6] Y.J. Feng, T. He, N. Alonso-Vante, Chem. Mater. 20 (2008) 26.
[7] R.W. Reeve, P.A. Christensen, A.J. Dickinson, A. Hamnett, K. Scott, Electrochim. Acta 45 (2000) 4237.
[8] C.W.B. Bezerra, L. Zhang, K.C. Lee, H.S. Liu, A.L.B. Marques, E.P. Marques, H.J. Wang, J.J. Zhang, Electrochim. Acta 53 (2008) 4937.
[9] K.P. Gong, F. Du, Z.H. Xia, M. Durstock, L.M. Dai, Science 323 (2009) 760.
[10] Y.F. Tang, B.L. Allen, D.R. Kauffman, A. Star, J. Am. Chem. Soc. 131 (2009) 13200.
[11] M. Zhou, Y.M. Zhai, S.J. Dong, Anal. Chem. 81 (2009) 5603.
[12] Y.R. Kim, S. Bong, Y.J. Kang, Y. Yang, R.K. Mahajan, J.S. Kim, H. Kim, Biosens. Bioelectron. 25 (2010) 2366.
[13] S.R.C. Vivekchand, C.S. Rout, K.S. Subrahmanyam, A. Govindaraj, C.N.R. Rao, J. Chem. Sci. 120 (2008) 9.
[14] F.H. Li, J.F. Song, H.F. Yang, S.Y. Gan, Q.X. Zhang, D.X. Han, A. Ivaska, L. Niu, Nanotechnology 20 (2009) 455602.
[15] C.Y. Wang, D. Li, C.O. Too, G.G. Wallace, Chem. Mater. 21 (2009) 2604.
[16] P. Guo, H.H. Song, X.H. Chen, Electrochem. Commun. 11 (2009) 1320.
[17] Z.Y. Yin, S.X. Wu, X.Z. Zhou, X. Huang, Q.C. Zhang, F. Boey, H. Zhang, Small 6 (2010) 307.
[18] Y. Wang, Y. Wan, D. Zhang, Electrochem. Commun. 12 (2010) 187.
[19] S. Bong, Y.R. Kim, I. Kim, S. Woo, S. Uhm, J. Lee, H. Kim, Electrochem. Commun. 12 (2010) 129.
[20] J. Sato, K. Higurashi, K. Fukuda, W. Sugimoto, Electrochemistry 79 (2011) 337.
[21] Y.J. Hu, H. Zhang, P. Wu, B. Zhou, C.X. Cai, Phys. Chem. Chem. Phys. 13 (2011) 4083.
[22] R. Kou, Y.Y. Shao, D.H. Wang, M.H. Engelhard, J.H. Kwak, J. Wang, V.V. Viswanathan, C.M. Wang, Y.H. Lin, Y. Wang, I.A. Aksay, J. Liu, Electrochem. Commun. 11 (2009) 954.
[23] F.H. Li, H.F. Yang, C.S. Shan, Q.X. Zhang, D.X. Han, A. Ivaska, L. Niu, J. Mater. Chem. 19 (2009) 4022.
[24] D.S. Geng, Y. Chen, Y.G. Chen, Y.L. Li, R.Y. Li, X.L. Sun, S.Y. Ye, S. Knights, Energy Environ. Sci. 4 (2011) 760.
[25] L.T. Qu, Y. Liu, J.B. Baek, L.M. Dai, ACS Nano 4 (2010) 1321.
[26] L.P. Zhang, Z.H. Xia, J. Phys. Chem. C 115 (2011) 11170.
[27] A.L.M. Reddy, A. Srivastava, S.R. Gowda, H. Gullapalli, M. Dubey, P.M. Ajayan, ACS Nano 4 (2010) 6337.
[28] Y. Wang, Y.Y. Shao, D.W. Matson, J.H. Li, Y.H. Lin, ACS Nano 4 (2010) 1790.
[29] L.S. Panchokarla, K.S. Subrahmanyam, S.K. Saha, A. Govindaraj, H.R. Krishna-murthy, U.V. Waghmare, C.N.R. Rao, Adv. Mater. 21 (2009) 4726.
[30] X.L. Li, H.L. Wang, J.T. Robinson, H. Sanchez, G. Diankov, H.J. Dai, J. Am. Chem. Soc. 131 (2009) 15939.
[31] J.J. Wu, Y. Wang, D. Zhang, B.R. Hou, J. Power Sources 196 (2011) 1141.
[32] Y. Wang, D. Zhang, H.Q. Liu, J. Power Sources 195 (2010) 3135.
[33] G.X. Wang, X.P. Shen, B. Wang, J. Yao, J. Park, Carbon 47 (2009) 1359.
[34] D. Li, M.B. Muller, S. Gilje, R.B. Kaner, G.G. Wallace, Nat. Nanotechnol. 3 (2008) 101.
[35] W.J. Zhou, D.D. Zhao, M.W. Xu, C.L. Xu, H.L. Li, Electrochim. Acta 53 (2008) 7210.
[36] L.B. Kong, M.C. Liu, J.W. Lang, M. Liu, Y.C. Luo, L. Kang, Solid State Electrochem. 15 (2011) 571.
[37] F. Tuinstra, J.L. Koening, J. Chem. Phys. 53 (1970) 1126.
[38] S. Stankovich, D.A. Dikin, R.D. Piner, K.A. Kohlhaas, A. Kleinhammes, Y. Jia, Y. Wu, S.T. Nguyen, R.S. Ruoff, Carbon 45 (2007) 1558.
[39] G.K. Ramesha, S. Sampath, Phys. Chem. C 113 (2009) 7985.
[40] H.L. Guo, X.F. Wang, Q.Y. Qian, F.B. Wang, X.H. Xia, ACS Nano 3 (2009) 2653.
[41] K. Tammeveski, K. Kontturi, R.J. Nichols, R.J. Potter, D.J. Schiffrin, J. Electroanal. Chem. 515 (2001) 101.
[42] M.N. Zhang, Y.M. Yan, K.P. Gong, L.Q. Mao, Z.X. Guo, Y. Chen, Langmuir 20 (2004) 8781.
[43] A. Sarapuu, K. Vaik, D.J. Schiffrin, K. Tammeveski, J. Electroanal. Chem. 541 (2003) 23.
[44] M. Lefevre, J.P. Dodelet, Electrochim. Acta 48 (2003) 2749.
[45] K.R. Lee, K.U. Lee, J.W. Lee, B.T. Ahn, S.I. Woo, Electrochem. Commun. 12 (2010) 1052.